Acta Pharmacologica Sinica (2018) 39: 213–221
 1671-4083/18
www.nature.com/aps

Article

D-*chiro*-inositol effectively attenuates cholestasis in bile duct ligated rats by improving bile acid secretion and attenuating oxidative stress

Shuang-shuang ZHAO[1, #], Na-ren LI[1, #], Wu-li ZHAO[1], Hong LIU[1], Mao-xu GE[1], Yi-xuan ZHANG[1], Long-yin ZHAO[2], Xue-fu YOU[3], Hong-wei HE[1, *], Rong-guang SHAO[1, *]

[1]*Key Laboratory of Biotechnology of Antibiotics, the National Health and Family Planning Commission (NHFPC); Department of Oncology, Institute of Medicinal Biotechnology, Chinese Academy of Medical Sciences and Peking Union Medical College, Beijing 100050, China;* [2]*Beijing Jince-Spring Medical Technology Co, Ltd, Beijing 100102, China;* [3]*Department of Pharmacology, Institute of Medicinal Biotechnology, Chinese Academy of Medical Sciences and Peking Union Medical College, Beijing 100050, China*

Abstract

Cholestatic liver diseases are important causes of liver cirrhosis and liver transplantation, but few drugs are available for treatment. D-*chiro*-inositol (DCI), an isomer of inositol found in many *Leguminosae* plants and in animal viscera, is used clinically for the treatment of polycystic ovary syndrome (PCOS) and diabetes mellitus. In this study, we investigated whether DCI exerted an anti-cholestatic effect and its underlying mechanisms. A cholestatic rat model was established via bile duct ligation (BDL). After the surgery, the rats were given DCI (150 mg·kg^{-1}·d^{-1}) in drinking water for 2 weeks. Oral administration of DCI significantly decreased the serum levels of alanine aminotransferase (ALT) and aspartate aminotransferase (AST), and attenuated bile duct proliferation, parenchymal necrosis and fibrosis in BDL rats. Furthermore, DCI treatment significantly increased the serum and bile levels of total bile acid (TBA), and decreased TBA levels in the liver. Moreover, DCI treatment significantly increased expression of the genes encoding bile acid transporters BSEP (Abcb11) and MRP2 (Abcc2) in liver tissues. DCI treatment also markedly decreased hepatic CD68 and NF-kappaB (NF-κB) levels, significantly decreased the serum and hepatic MDA levels, markedly increased superoxide dismutase activity in both serum and liver tissues. Using whole-genome oligonucleotide microarray, we revealed that DCI treatment altered the expression profiles of oxidation reduction-related genes in liver tissues. Collectively, DCI effectively attenuates BDL-induced hepatic bile acid accumulation and decreases the severity of injury and fibrosis by improving bile acid secretion, repressing inflammation and decreasing oxidative stress. The results suggest that DCI might be beneficial for patients with cholestatic disorders.

Keywords: d-*chiro*-inositol; cholestatic liver diseases; bile duct ligation; liver fibrosis; bile acid transporters; inflammation; oxidative stress

Acta Pharmacologica Sinica (2018) 39: 213–221; doi: 10.1038/aps.2017.98; published online 27 Jul 2017

Introduction

Cholestasis is typically characterized as the presence of bile within hepatocytes and canalicular spaces in association with generalized cholate injury, which is a symptom of many types of liver disease. Chronic cholestasis results in liver necrosis, fibrosis, cirrhosis, and eventual liver failure necessitating liver transplantation[1-3]. Cholestasis often does not respond to medical therapy. Ursodeoxycholic acid (UDCA), one of the few drugs currently used in the clinic to manage cholestasis, produces only limited results on select types of the disease[4]. Therefore, alternative beneficial treatments for cholestasis must be developed to improve the management and prognosis of patients with liver disease.

D-*chiro*-inositol (DCI), an isomer of inositol, is found in many *Leguminosae* plants and in animal viscera. DCI has been used clinically for the treatment of polycystic ovary syndrome (PCOS) and diabetes mellitus, owing to its insulin-like bioactivity[5-7]. DCI also exhibits anti-oxidative, anti-inflammatory and anti-aging effects[8, 9]. Additionally, DCI showed hepatoprotective and anti-oxidative effects in mice fed a high-fructose diet: mice treated with DCI showed improvements in liver function; serum lipid profile; ALT, AST, LDH and CRP levels in serum; and MDA, T-SOD and GSH-Px levels in

# These authors contributed equally to this work.
*To whom correspondence should be addressed.
E-mail hehwei@imb.pumc.edu.cn (Hong-wei HE);
shaor@imb.pumc.edu.cn (Rong-guang SHAO)
Received 2016-12-12 Accepted 2017-03-30

hepatic tissue[9].

The present study was designed to assess how DCI affects liver fibrosis in rats with bile duct ligation (BDL). To accomplish this objective, we created a cholestatic liver fibrosis model through BDL and used this model to identify the potential mechanisms underlying DCI's effects. Overall, our results support the therapeutic use of DCI for hepatic injury and fibrosis.

Materials and methods

Chemicals and reagents

DCI was produced by Beijing Jince-Spring Medical Technology Co, Ltd. Sirius Red (Direct Red 80, 365548) was purchased from Sigma (St Louis, MO, USA). Antibodies against BSEP (sc-74500) and CD68 (sc-9139) were purchased from Santa Cruz Biotechnology (Dallas, TX, USA), antibodies against MRP2 (ab172630) were purchased from Abcam (Cambridge, UK), and antibodies against NF-κB (8242) were purchased from Cell Signaling Technology (Beverley, MA, USA). Hydroxyproline (HYP), malondialdehyde (MDA), superoxide dismutase (SOD) and total bile acid (TBA) assay kits were purchased from Nanjing Jiancheng Bioengineering Institute (Nanjing, China). Alanine aminotransferase (ALT), aspartate aminotransferase (AST), total bilirubin (TBIL), total cholesterol (CHO), high-density lipoprotein (HDL) cholesterol, and low-density lipoprotein (LDL) cholesterol kits were purchased from Zhongsheng Beikong Biotechnology (Beijing, China). A nucleoSpin RNA clean-up kit was purchased from Macherey-Nagel (Germany), Cy3/Cy5 labeling kits were purchased from Genesphere Inc (Hatfield, PA, USA), and Rat OneArray® microarrays were purchased from Phalanx Biotech Group (Taiwan, China).

Animal experiments

Fifteen adult male Sprague-Dawley rats (180–220 g) were provided by the Laboratory Animal Center of the Academy of Military Medical Sciences in Beijing. The rats were randomly divided into three groups (n=5 per group): the sham-operated group, the BDL group and the BDL-DCI group. The rats in the BDL and BDL-DCI groups underwent a common BDL operation, in which the common bile duct was identified and doubly ligated using 5-0 silk sutures. For the two ligatures, one was made below the junction of the hepatic ducts, and the other was made above the entrance to the pancreatic ducts; the common bile duct was resected between them. For the sham operation, a midline incision was made in the abdomen and then closed. The sham-operated group served as the healthy control group. At 24 h after surgery, the rats in the BDL-DCI group were given free access to drinking water supplemented with 1.5 mg/mL DCI for 14 d, whereas the rats in the sham and BDL groups were given free access to drinking water with no DCI. Body weight was measured daily. At the end of the 2-week treatment period, serum, bile, urine and liver samples were collected for further analyses, as previously described[10]. All animal experiments were approved by the Institutional Animal Care and Use Committee of the Institute of Medicinal Biotechnology, Chinese Academy of Medical Sciences.

Serum, urine, bile and liver tissue biochemistry

A Hitachi 7170 chemistry analyzer was used to measure serum ALT, AST, TBIL, total CHO, HDL cholesterol and LDL cholesterol levels and urine and bile TBIL levels. The HYP and MDA content and SOD enzyme activity in the liver tissue were detected as previously described[11].

Liver histology

Formalin-fixed liver tissue was embedded in paraffin, and sections were stained with hematoxylin and eosin (H&E) and Sirius red. Histological evaluation of the liver sections was performed in a double-blinded manner, and bile duct proliferation and necrosis were assessed on a 1 to 5+ scale. Sirius red-stained sections were photographed with a Leica DM1000 microscope, and 6 images in each section were randomly taken to quantify the Sirius red staining using a Leica Qwin V3 system. The average area% of the 6 districts was used to evaluate the fibrosis level.

Immunohistochemical evaluation

Liver tissue sections underwent pretreatment for antigen retrieval using citrate and the removal of endogenous catalase, as previously described[11]. Then, the sections were incubated overnight at 4 °C with mouse anti-CD68 (1:50) or rabbit anti-NF-κB (1:500) monoclonal antibodies, washed and incubated with secondary antibodies for 20 min at 37 °C. The color was developed by incubation with 3,3N-diaminobenzidine tetrahydrochloride for 2–5 min. The images were recorded with light microscopy. Quantitation of CD68 and NF-κB labeling was performed using ImageJ software (NIH open source) with thresholding. The data are presented as a percentage of the total area that was positive for CD68 and NF-κB.

qRT-PCR analysis

Total RNA was extracted from liver tissues using TRIzol (Invitrogen) and purified using a NucleoSpin RNA Clean-up kit (Macherey-Nagel, Duren, Germany). Complementary DNA was generated using a Transcriptor First-strand cDNA Synthesis kit (Roche), and the relative expression of specific genes was detected using TaqMan real-time PCR. The GAPDH gene was used as a reference to normalize data.

Western blotting

Western blotting assays were performed using whole liver lysates of the liver samples, as described previously[12]. The gel band intensity was quantified using Alphaview-FluorChem HD2 (V3.4, Proteinsimple, San Jose, CA, USA) and normalized to GAPDH.

Whole-genome oligonucleotide microarray analysis

Total RNA was isolated from liver tissue using TRIzol reagent (Invitrogen) and purified using a NucleoSpin RNA clean-up kit. An RNA sample was pooled for each group by mixture of the same amount of total RNA from each animal in the group.

The samples were then labeled with Cy3 and Cy5 during a reverse transcription process using Cy3/Cy5 labeling kits (Genesphere) according to the manufacturer's instructions. The labeled DNA was hybridized with microarrays overnight at 45 °C. After hybridization and subsequent washing, the arrays were analyzed using a LuxScan 10K/A dual-channel laser scanner (CapitalBio, Beijing). The data were normalized using the Lowess method, and only genes that exhibited a consistent alteration tendency (both ≥1.5-fold) in both microarrays were selected as differentially expressed genes. A gene-function analysis was performed using DAVID Bioinformatics Resources (The Database for Annotation, Visualization and Integrated Discovery)[13, 14].

Statistical analysis

The data are presented as the mean±standard deviations. Two-tailed Student's *t*-tests were used to assess differences between the experimental groups. Statistical significance was set at $P<0.05$.

Results

Effects of DCI on serum, urine and bile biochemistry in BDL rats

To evaluate the effects of DCI on BDL rats, serum, urine and bile biochemistry were analyzed (Table 1). Serum levels of ALT and AST were elevated by 4.3- and 8.3-fold, respectively, in the BDL rats ($P<0.01$); both were significantly decreased by 38.8% and 34.8%, respectively, after DCI treatment ($P<0.01$). There were no significant differences in TBIL, CHO, LDL or HDL after DCI treatment. These data indicated that DCI significantly attenuates liver injury but has no effect on lipid metabolism.

DCI improved hepatic pathology in BDL rats

The hematoxylin and eosin staining results showed that the rats in the sham-operated group had normal liver morphology with intact hepatocytes and portal tracts (Figure 1A). In contrast, the hepatic pathology of the BDL rats exhibited marked changes, including parenchymal necrosis and an abundance of newly formed bile ducts (Figure 1B). The rats in the BDL-DCI group showed markedly improved hepatic pathology compared with that in the BDL rats (Figure 1C). A double-blinded assessment revealed that bile duct proliferation and parenchymal necrosis significantly declined in the BDL-DCI rats by 42.1% and 50.6%, respectively, compared with that in the BDL rats (Figure 1D and 1E). These data indicated that DCI improves BDL-induced hepatic pathological changes by decreasing bile duct proliferation and necrosis.

DCI alleviated BDL-induced liver fibrosis

Sirius red staining is a classical histopathological technique for the observation of collagen. In this study, the Sirius red results showed marked collagen deposition in the BDL rats at the end of the two-week experimental period (Figure 2B). However, DCI supplementation significantly attenuated collagen accumulation, as shown by the 37.4% decrease in the Sirius red staining area ($P<0.05$, Figure 2D). The extent of liver fibrosis was confirmed by measuring the hepatic hydroxyproline concentration, and DCI treatment was found to significantly decrease the hydroxyproline content, by 22.6% ($P<0.05$, Figure 2E). These observations suggested that DCI has an anti-fibrotic effect on cholestatic liver injury in BDL rats.

DCI improved bile acid secretion in BDL rat livers

Bile acid concentrations were measured in serum, urine, bile and liver tissue routinely in our BDL experiments. Concentrations of TBA in serum, urine and liver tissues were markedly increased in the BDL rats, a result consistent with findings from previous BDL experiments[10-12, 15]. Surprisingly, DCI treatment increased TBA levels in serum and bile and significantly decreased TBA content in liver tissue (Figure 3A). These data indicated that DCI may promote liver secretion of TBA into the bile and serum in BDL rats.

The expression of genes encoding bile acid transporters in the liver was further analyzed. The results showed that DCI partially reversed BDL-mediated repression of BSEP (Abcb11) and MRP2 (Abcc2) mRNA and protein expression (Figure 3B–3D). These changes may have promoted the secretion of bile acid from hepatocytes into bile ducts, thus resulting in

Table 1. Serum, urine, and bile biochemistry in BDL rats.

	Sham	BDL	BDL-DCI
Serum ALT (U/L)	25.25±1.26	107.80±15.77$^{\#\#}$	66.00±21.38**
Serum AST (U/L)	91.00±20.02	754.20±65.06$^{\#\#}$	491.40±103.36**
Serum TBIL (μmol/L)	0.15±0.10	132.92±15.62$^{\#\#}$	139.56±9.71
Serum total CHO (mmol/L)	1.78±0.44	2.28±0.58	2.66±0.17
Serum LDL (mmol/L)	0.28±0.11	1.08±0.36$^{\#\#}$	1.29±0.28
Serum HDL (mmol/L)	1.20±0.28	0.25±0.09$^{\#\#}$	0.35±0.06
Urine TBIL (μmol/L)	0.225±0.45	97.16±60.96$^{\#}$	59.18±15.52
Bile TBIL (μmol/L)	No applicable	175.43±110.46	152.33±85.33

Data are expressed as the mean±SD with $n=5$ per group. ALT, alanine aminotransferase; AST, aspartate aminotransferase; TBIL, total bilirubin; CHO, cholesterol; LDL, low-density lipoprotein; HDL, high-density lipoprotein; TBA, total bile acid. $^{**}P<0.01$ *vs* BDL alone group. $^{\#}P<0.05$, $^{\#\#}P<0.01$ *vs* sham control group.

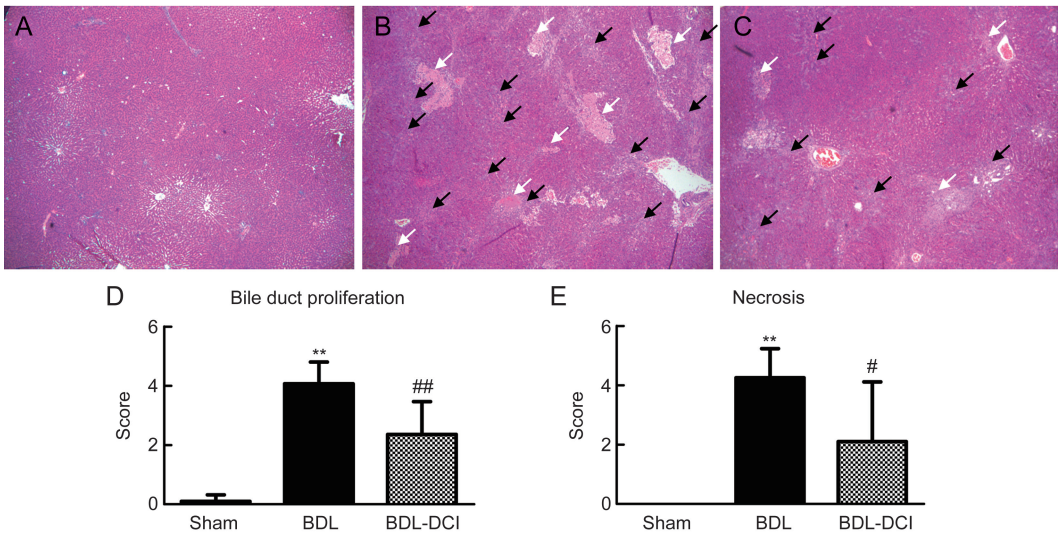

Figure 1. DCI improved hepatic histopathology in BDL rats. Liver sections were stained with hematoxylin & eosin (×40). (A) Sham group; (B) BDL group; (C) BDL-DCI (150 mg/kg) group. Black arrows indicate ductular proliferation areas; white arrows indicate necrosis areas. Blinded quantitative assessments of (D) bile duct proliferation and (E) necrosis were conducted; the scores are expressed as the mean±SD, $^{**}P<0.01$ *vs* the sham group. $^{\#}P<0.05$ and $^{\#\#}P<0.01$ *vs* the BDL group. $n=5$ per group.

decreased bile acid concentration in liver tissues.

DCI attenuated BDL-induced inflammation

Inflammatory cell infiltration and NF-κB activation occur during prolonged biliary obstruction, thereby promoting the development of liver fibrosis. Immuno-histochemical staining of CD68 and NF-κB was used to evaluate the effect of DCI on inflammation induced by BDL. The results revealed that CD68 expression and NF-κB activation were dramatically elevated in liver tissue after BDL. However, DCI treatment markedly lowered the protein levels of NF-κB and CD68 (Figure 4). These data suggested that DCI attenuates the inflammation induced by BDL in rats.

DCI attenuated BDL-induced oxidative stress

MDA is one of the most important products of lipid peroxidation. The MDA concentration was measured in both serum and liver tissue. The BDL rats exhibited increased MDA levels in both serum and liver tissue, and DCI treatment decreased these levels by 31.2% ($P<0.05$) and 32.9% ($P<0.05$), respectively

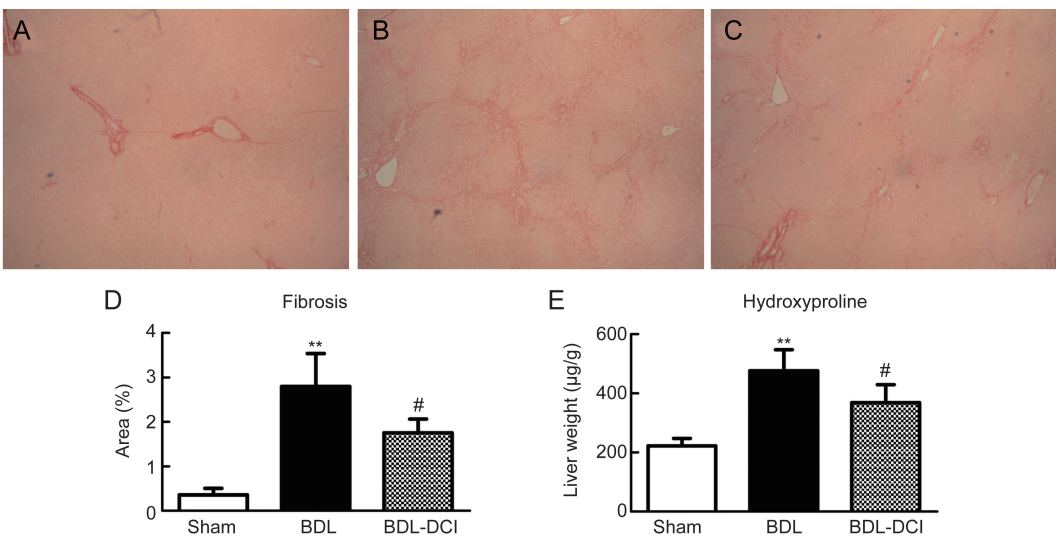

Figure 2. DCI alleviated BDL-induced liver fibrosis. The obtained liver sections were stained with Sirius red (×40). (A) Sham group; (B) BDL group; (C) BDL-DCI (150 mg/kg) group. (D) DCI treatment markedly decreased the presence of collagen fiber; area% is shown. (E) The content of hydroxyproline in liver tissue was detected, and DCI treatment significantly decreased this parameter. Values are expressed as the mean±SD. $^{**}P<0.01$ *vs* the sham group; $^{\#}P<0.05$ *vs* the BDL group. $n=5$ per group.

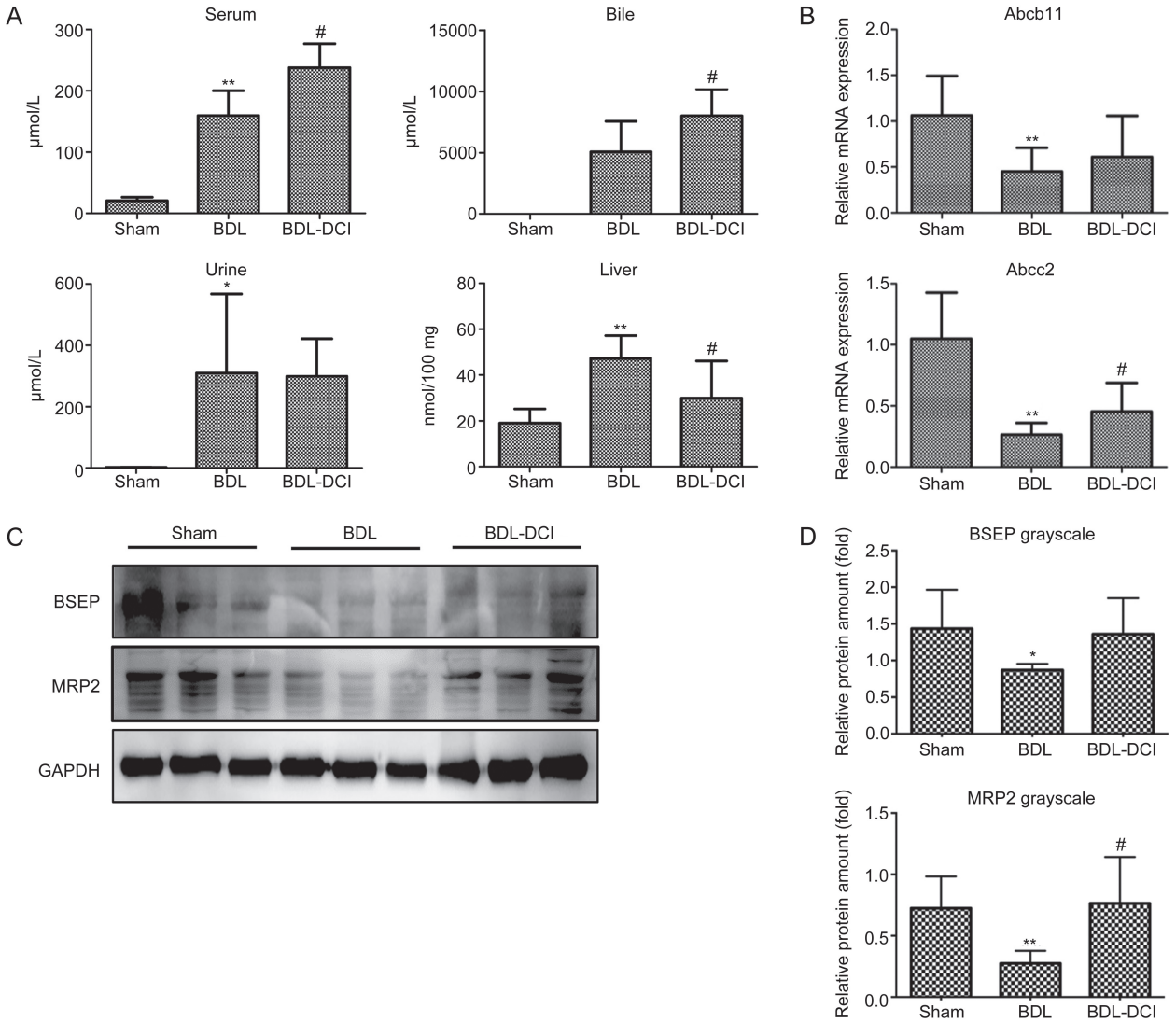

Figure 3. DCI altered the bile acid distribution and gene expression patterns in BDL rats. (A) Bile acid concentrations in the serum, bile, urine and liver tissue. (B) mRNA and (C) protein expression levels of BSEP (Abcb11) and MRP2 (Abcc2) were detected in the liver. (D) The Western blotting results for each animal are quantified in the three groups. Values are expressed as the mean±SD. $^{**}P<0.01$ *vs* the sham group; $^{\#}P<0.05$ *vs* the BDL group. $n=5$ per group.

(Figure 5A and 5C). The activity of SOD reflects the capacity to remove free radicals. In both serum and liver tissue, SOD activity was decreased in the BDL rats, but the activity was markedly increased after DCI treatment (Figure 5B and 5D). These data indicated that DCI attenuates BDL-induced oxidative stress.

DCI altered gene expression profiles in BDL rat livers

To analyze genome-wide alterations in gene expression, total RNA was extracted from rat liver tissue samples for the microarray experiments. For our analysis, an alteration of 1.5-fold in signal intensity was regarded as a significant change in mRNA expression. Overall, 25 genes were up-regulated in the BDL rats and down-regulated in the BDL-DCI group, whereas 56 genes were down-regulated in the BDL rats and up-regulated in the BDL-DCI group. These 81 genes were clustered using a hierarchical average-linkage clustering program as described previously[16] and were further characterized with gene functional enrichment analysis using DAVID Bioinformatics Resources. The results showed that 14 genes were included in the term 'oxidation reduction'; these included Wfdc21, Kng1, Kng1l1, Cyp2d1, Rdh2, Cyp4a1, UST4r, Nsbp1, Rup-4, Cyp2d5, Sult1e1, Sult1c2a, Sult2a2, and Ces1d (Figure 6). These data further confirmed that DCI attenuates BDL-induced oxidative stress.

Discussion

When untreated, cholestatic liver disease progresses to liver cirrhosis and end-stage liver disease and is thus a frequent cause for liver transplantation (~15%)[17]. The accumulation of toxic bile acids in the liver is an important cause of chronic cholestasis, which leads to liver necrosis, fibrosis, and

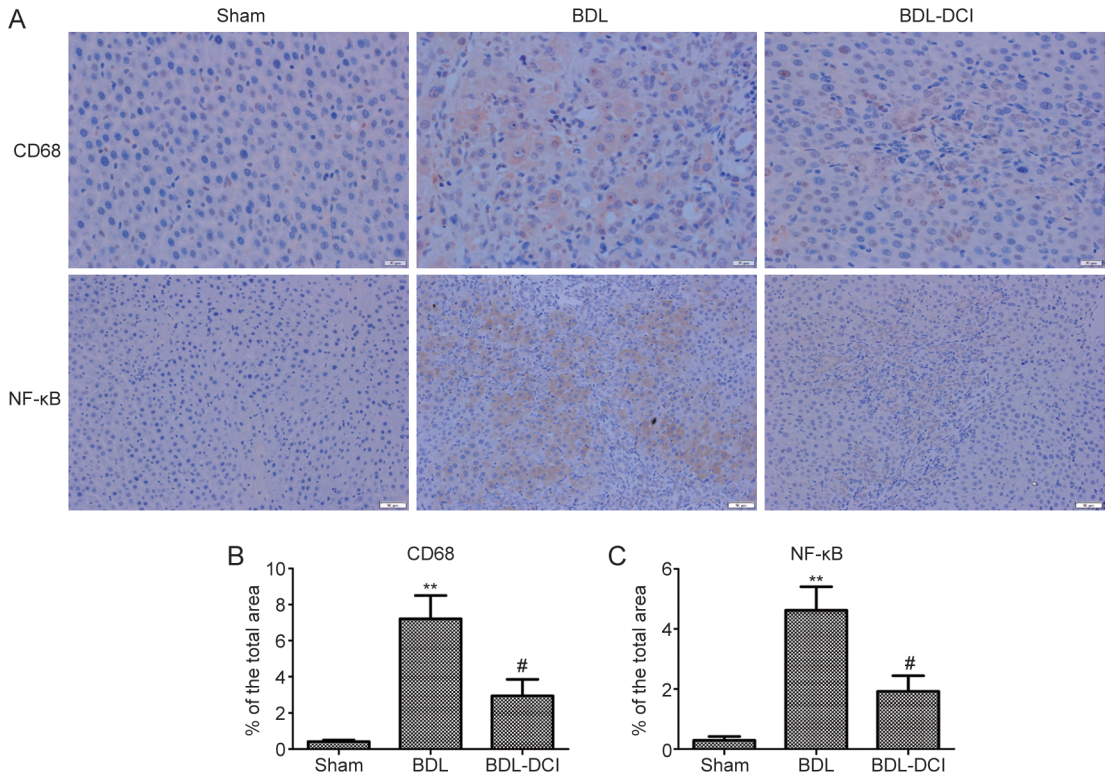

Figure 4. DCI suppressed liver inflammation in BDL rats. (A) Liver tissue sections were subjected to immunohistochemical examination with antibodies against CD68 (×400) and NF-κB (×200). The quantification of (B) CD68; (C) NF-κB revealed DCI suppressed liver inflammation. $^{**}P<0.01$ *vs* sham group; $^{\#}P<0.05$ *vs* BDL group. *n*=5 per group.

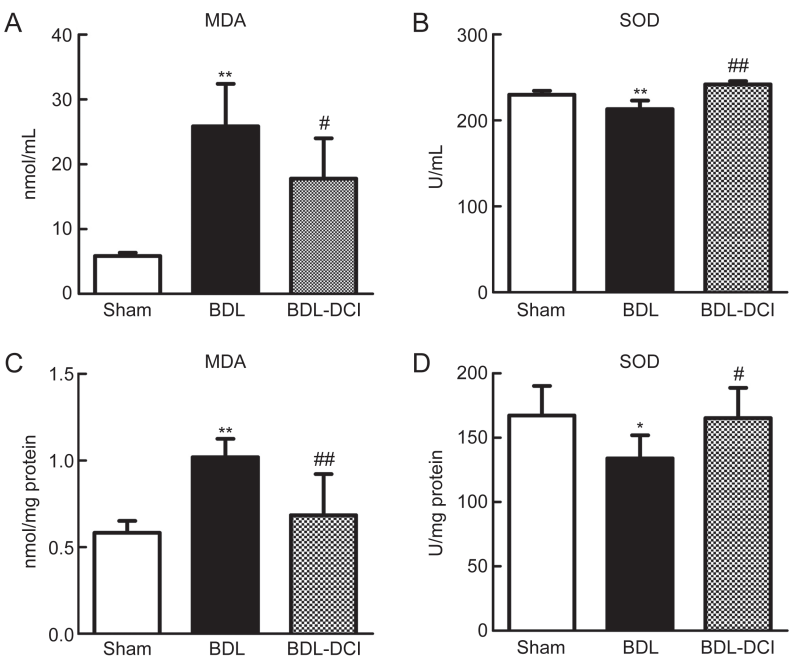

Figure 5. DCI attenuated BDL-induced oxidative stress. Levels of the lipid peroxidation product MDA and SOD activity were measured in serum (A and B) and liver tissue (C and D). Quantitative data are expressed as the mean±SD. $^{*}P<0.05$ and $^{**}P<0.01$ *vs* sham group; $^{\#}P<0.05$ and $^{\#\#}P<0.01$ *vs* BDL group. *n*=5 per group.

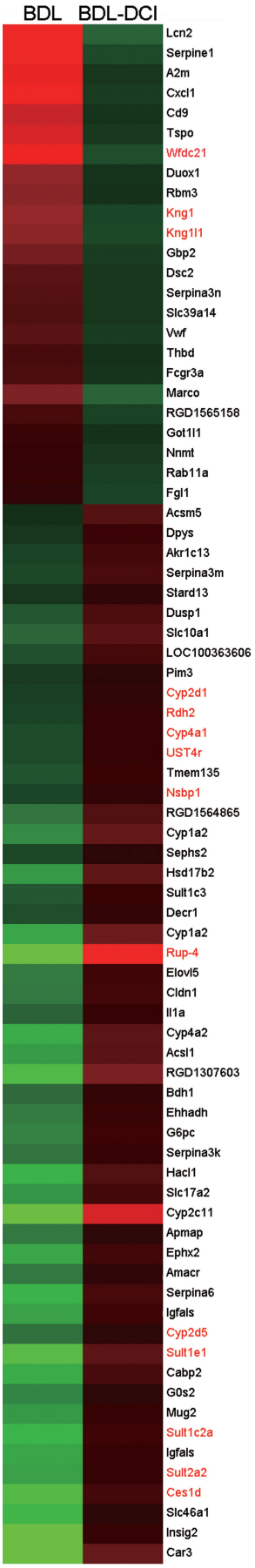

Figure 6. Cluster analysis of gene expression changes measured by microarray analysis. Red: increase in gene expression; green: decrease in gene expression. The highlighted gene symbols represent significantly changed genes included in the term 'oxidation reduction' and identified using DAVID Bioinformatics Resources.

cirrhosis[18].

In this study, we assessed the hepato-protective and anti-fibrotic effects of DCI in BDL rats and analyzed the role of this compound in regulating bile acid distribution and liver genome expression in these rats.

Prior *in vivo* studies have demonstrated the hepatoprotective effect of DCI-enriched tartary buckwheat extract in mice fed a high-fructose diet, as evidenced by decreases in serum ALT and AST activity and in other serum biochemical indices[9]. In the present study, DCI decreased serum ALT (P<0.05) and AST activity (P<0.05) and decreased the TBA content in liver tissue (P<0.05). Furthermore, hematoxylin and eosin staining results showed that DCI markedly improved the hepatic histopathology in BDL rats. Notably, bile duct proliferation and parenchymal necrosis were clearly attenuated after treatment with DCI. These results suggested that DCI exerts hepatoprotective effects on BDL-induced liver injury in rats.

Hepatic fibrosis refers to the excessive deposition of 'scar' extracellular matrix, particularly types I and III collagen, as a result of either acute or chronic liver injury[19]. We assessed the effect of DCI on hepatic fibrosis by Sirius red staining, which stains fibroplasia and abnormal collagen fibers dark red-brown. Our results showed that DCI decreased the percentage of positively stained areas (P<0.05). To confirm the anti-liver-fibrosis effect of DCI, we also measured the liver hydroxyproline content, which is the current gold standard for detecting the extent of liver fibrosis. We found that DCI decreased the content of hydroxyproline in the livers of the BDL rats (P<0.05). We concluded that DCI inhibits fibrogenesis, a finding that has not previously been reported.

Bile acid accumulation is the major pathological inducer in BDL animals; thus, such accumulation validated our successful creation of an accurate BDL model. In this study, DCI repressed bile acid accumulation in the liver (P<0.05), thereby decreasing liver injury and fibrogenesis. Further gene analysis revealed that DCI treatment partially reversed the down-regulation of MRP2 (P<0.05) and BSEP. MRP2 and BSEP are important transporters at the apical (canalicular) membranes of hepatocytes and facilitate bile acid secretion from hepatocytes into bile ducts[20]. These data are consistent with the results showing that the bile acid concentration in the bile of the DCI-treated animals was significantly higher than that in the untreated animals. Transporters at the basolateral membrane of hepatocytes such as OATPs and MRP3 were also analyzed but showed no significant changes (data not shown), thus indicating that the observed increases in serum bile acid concentration may not have been directly from the liver.

Inflammation and immune responses are important elements in the initiation and progression of liver fibrosis, and Kupffer cells, the tissue-specific macrophage population in the liver, are key effector cells in the liver inflammatory response[19]. Kupffer cells signal though NF-κB activation to express several inflammatory mediators and regulate the inflammatory response[21, 22]. We used immunohistochemical staining of CD68, a marker of Kupffer cells, and NF-κB to assess the effects of DCI on inflammation in BDL rats. Our

results showed that DCI treatment noticeably decreased CD68 and NF-κB expression, thus indicating that DCI inhibited the accumulation of Kupffer cells and suppressed the inflammatory response in these rats. Conjugated bile acids increase the activation of nuclear factor-kappa B (NF-κB)[23]; in this study, bile acids were increased in BDL rat livers and decreased in DCI-treated BDL rat livers through improving bile acid secretion, thus indicating that this process might be part of the anti-inflammatory mechanism of DCI in the rats.

Enhanced oxidative stress contributes to hepatic fibrogenesis, owing to its promotion of HSC activation, apoptosis and recruitment of inflammatory cells[24]. The development of oxidative stress is associated with increased levels of reactive oxygen species, including superoxide, hydrogen peroxide and a variety of harmful products[25]. We detected the content of MDA, an important lipid peroxidation product, and the activity of SOD, which reflects the capacity to remove free radicals, in both the serum and liver tissue in BDL rats. DCI was shown to be a powerful anti-oxidant by decreasing MDA content and increasing SOD activity in both serum and liver tissue after BDL. Gene expression profiling also showed that DCI treatment altered the expression of a collection of genes related to oxidation reduction. Thus, it can be deduced that DCI protects the liver in part by attenuating BDL-induced oxidative stress.

In summary, DCI showed a significant therapeutic effect in a rat model of cholestasis. This effect might have arisen from the improvement of bile acid secretion and the repression of liver inflammation and oxidative stress. These findings suggest that DCI might be beneficial for patients with cholestatic disorders.

Conflicts of interest

The authors have submitted a Chinese patent, and the patent has been issued by the patent agency. The patent number is 201610112806.9. Co-author Long-yin ZHAO is an employee at Beijing Jince-Spring Medical Technology Co, Ltd, which provided the drug DCI.

Acknowledgements

This work was supported by the CAMS Innovation Fund for Medical Sciences (CIFMS) (2016-I2M-2-002), the National Natural Science Foundation of China (81673497 and 81473249), the National Mega-project for Innovative Drugs (2014ZX09201042), and the Beijing Natural Scientific Foundation (7162130).

Author contribution

Hong-wei HE, Rong-guang SHAO and Long-yin ZHAO designed the research project; Shuang-shuang ZHAO, Na-ren LI, Wu-li ZHAO, Hong LIU, Mao-xu GE, Yi-xuan ZHANG and Xue-fu YOU performed the experiment; Shuang-shuang ZHAO and Na-ren LI analyzed the data; Long-yin ZHAO provided the drug DCI; Hong-wei HE, Xue-fu YOU and Rong-guang SHAO contributed the reagents and other materials; and Shuang-shuang ZHAO, Na-ren LI and Hong-wei HE wrote the manuscript.

References

1 Trauner M, Meier PJ, Boyer JL. Molecular pathogenesis of cholestasis. New Engl J Med 1998; 339: 1217–27.
2 Scheiman JM, Moseley RH. Cholestasis. Compr Ther 1994; 20: 28–35.
3 Wagner M, Trauner M. Recent advances in understanding and managing cholestasis. F1000Res 2016; 5. pii: F1000 Faculty Rev-705.
4 Chapman RW. High-dose ursodeoxycholic acid in the treatment of primary sclerosing cholangitis: throwing the urso out with the bathwater? Hepatology 2009; 50: 671–3.
5 Gao YF, Zhang MN, Wang TX, Wu TC, Ai RD, Zhang ZS. Hypoglycemic effect of D-*chiro*-inositol in type 2 diabetes mellitus rats through the PI3K/Akt signaling pathway. Mol Cell Endocrinol 2016; 433: 26–34.
6 Lagana AS, Barbaro L, Pizzo A. Evaluation of ovarian function and metabolic factors in women affected by polycystic ovary syndrome after treatment with D-*Chiro*-Inositol. Arch Gynecol Obstet 2015; 291: 1181–6.
7 Cianci A, Panella M, Fichera M, Falduzzi C, Bartolo M, Caruso S. d-*chiro*-Inositol and alpha lipoic acid treatment of metabolic and menses disorders in women with PCOS. Gynecol Endocrinol 2015; 31: 483–6.
8 Hada B, Yoo MR, Seong KM, Jin YW, Myeong HK, Min KJ. D-*chiro*-inositol and pinitol extend the life span of *Drosophila melanogaster*. J Gerontol A Biol Sci Med Sci 2013; 68: 226–34.
9 Hu Y, Zhao Y, Ren D, Guo J, Luo Y, Yang X. Hypoglycemic and hepatoprotective effects of D-*chiro*-inositol-enriched tartary buckwheat extract in high fructose-fed mice. Food Funct 2015; 6: 3760–9.
10 He H, Mennone A, Boyer JL, Cai SY. Combination of retinoic acid and ursodeoxycholic acid attenuates liver injury in bile duct-ligated rats and human hepatic cells. Hepatology 2011; 53: 548–57.
11 Zhao S, Li N, Zhen Y, Ge M, Li Y, Yu B, *et al*. Protective effect of gastrodin on bile duct ligation-induced hepatic fibrosis in rats. Food Chem Toxicol 2015; 86: 202–7.
12 Yu DK, Zhang CX, Zhao SS, Zhang SH, Zhang H, Cai SY, *et al*. The anti-fibrotic effects of epigallocatechin-3-gallate in bile duct-ligated cholestatic rats and human hepatic stellate LX-2 cells are mediated by the PI3K/Akt/Smad pathway. Acta Pharmacol Sin 2015; 36: 473–82.
13 Huang da W, Sherman BT, Lempicki RA. Systematic and integrative analysis of large gene lists using DAVID bioinformatics resources. Nat Protoc 2009; 4: 44–57.
14 Huang DW, Sherman BT, Tan Q, Kir J, Liu D, Bryant D, *et al*. DAVID Bioinformatics Resources: expanded annotation database and novel algorithms to better extract biology from large gene lists. Nucleic Acids Res 2007; 35(Web Server issue): W169–75.
15 Zhen YZ, Li NR, He HW, Zhao SS, Zhang GL, Hao XF, *et al*. Protective effect of bicyclol against bile duct ligation-induced hepatic fibrosis in rats. World J Gastroenterol 2015; 21: 7155–64.
16 Zhao W, He H, Ren K, Zhang H, Chen Y, Shao RG. Myofibrillogenesis regulator-1 promotes cell adhesion and migration in human hepatoma cells. Chin Sci Bull 2013; 58: 3007–14.
17 O'Leary JG, Lepe R, Davis GL. Indications for liver transplantation. Gastroenterology 2008; 134: 1764–76.
18 Heathcote EJ. Diagnosis and management of cholestatic liver disease. Clin Gastroenterol Hepatol 2007; 5: 776–82.
19 Guo J, Friedman SL. Hepatic fibrogenesis. Semin Liver Dis 2007; 27: 413–26.
20 Boyer JL. Bile formation and secretion. Compr Physiol 2013; 3: 1035–78.

21 Tomita K, Tamiya G, Ando S, Ohsumi K, Chiyo T, Mizutani A, *et al*. Tumour necrosis factor alpha signalling through activation of Kupffer cells plays an essential role in liver fibrosis of non-alcoholic steatohepatitis in mice. Gut 2006; 55: 415–24.
22 Luedde T, Schwabe RF. NF-kappaB in the liver–linking injury, fibrosis and hepatocellular carcinoma. Nat Rev Gastroenterol Hepatol 2011; 8: 108–18.
23 Jones H, Alpini G, Francis H. Bile acid signaling and biliary functions. Acta Pharm Sin B 2015; 5: 123–8.
24 Bataller R, Brenner DA. Liver fibrosis. J Clin Invest 2005; 115: 209–18.
25 Kisseleva T, Brenner DA. Role of hepatic stellate cells in fibrogenesis and the reversal of fibrosis. J Gastroenterol Hepatol 2007; 22: S73–8.